ON PHOTOSPHERIC FLOWS AND CHROMOSPHERIC CORKS

P. N. BRANDT
Kiepenheuer-Institut für Sonnenphysik, Freiburg, Germany

R.J. RUTTEN
Sterrekundig Instituut, Utrecht, The Netherlands

R.A. SHINE
Lockheed Palo Alto Research Laboratories, Palo Alto, USA

and

J. TRUJILLO BUENO
Instituto de Astrofisica de Canarias, La Laguna, Tenerife, Spain

Abstract. Proper motions of granules are measured by local correlation tracking on a 4.5 h image sequence obtained with the Swedish Vacuum Tower Telescope at La Palma. A 2 arcsec spatial low-pass filter is applied to obtain meso-scale flow patterns. We find that their characteristic lifetime ($1/e$ value) has a lower limit of five to six hours. Comparison with a simultaneous co-spatial sequence of chromospheric Ca II K_{2V} images shows that these flows sweep supergranulation cells clean in about the same period. A chromospheric "persistent flasher", seen during three hours in Ca II K_{2V}, migrates to the magnetic network as if it were a photospheric cork.

Key words: solar convection, solar photosphere, solar chromosphere, mesogranulation

1. Introduction

The existence and properties of meso-scale flow patterns in the solar photosphere have been a matter of controversy for well over a decade. After their first detection and description by November *et al.* (1981), their existence was doubted by Damé (1985) and Damé and Martić (1987), who attributed them to waves on the basis of chromospheric phase patterns seen in Ca II K_{2V} filtergrams, and by Wang (1989). Others noted meso-scale variations in various types of photospheric structure (*e.g.*, Kawaguchi, 1980; Oda, 1984; Koutchmy and Lebecq, 1986; Dialetis *et al.*, 1988; Brandt *et al.*, 1991; Muller *et al.*, 1990) that may or may not confirm the existence of convection on a specific meso-size scale, perhaps corresponding to the depth of the He I ionization zone as proposed originally by Simon and Leighton (1964).

A new era in meso-scale studies came with the advent of the "local correlation tracking" software technique to determine horizontal flows by tracing proper motions of individual granules on granulation image sequences, sequentially while they come and go (November and Simon, 1988; Simon *et al.*, 1988; Brandt *et al.*, 1988; Title *et al.*, 1989). Meso-scale structure was found to be definitely present in these horizontal flows, characterized by cells of 4–10 arcsec diameter and velocities of order 0.4 km s^{-1}. Re-analysis of older spectroscopic data by Deubner (1989a, 1989b) confirmed their convective nature. Deubner questioned a direct connection with Ca II K_{2V} phase patterns, attributing these to p–mode interaction.

R. J. Rutten and C. J. Schrijver (eds.), Solar Surface Magnetism, 251–259.

However, a recent spectroscopic investigation by Straus *et al.* (1992), using two-dimensional observations to obtain high statistical significance, indicates that there is no clear separation between the granular velocity field and meso-scale radial velocity patterns in the photosphere. Higher up in the atmosphere, Straus *et al.* (1992) attribute the observed meso-scale patterning of radial velocity amplitudes to gravity waves excited by overshoot of only the largest granules.

Absence of a definite meso-scale implies that all parameters such as velocities, lifetimes, transport characteristics, *etc.* depend on the type of spatial low-pass filter applied to the data, so that speaking of "photospheric meso-granulation" makes sense only when one specifies precisely which spatial scales one refers to. It is not clear whether such absence of a particular scale in the meso regime holds also for horizontal flows. In particular, long-lived vorticity as found by Brandt *et al.* (1988) and other persistencies may operate on preferred horizontal scales.

In this contribution, we display results from La Palma data (Sect. 2). We first discuss horizontal meso-scale flows in the photosphere (Sect. 3), and then show that these are tracked by actual features in the chromosphere (Sect. 4).

2. Observations and analysis

We use a 4.5 h sequence of simultaneous granulation and Ca II K_{2V} images taken on June 27, 1990 with the Swedish Vacuum Solar Telescope on La Palma. For the granulation images, a narrow-band (FWHM 10 Å) interference filter transmitted the G band at $\lambda = 4308$ Å to a COHU video camera. It registered a field of 41×36 arcsec^2 with a pixel size of 0.17 arcsec. The best video frames (or at least, the better ones) were selected in real time for 8-bit digitization and disk storage by biological image-grabber systems, consisting of three of the authors who alternated in monitoring the live image under control of the fourth. This resulted in a series of 1549 selected frames at somewhat irregular (but accurately documented) time intervals of 10.2 s average. The sequence is of good quality, permitting local correlation tracking of granules over its entire duration.

The Ca II K_{2V} images were digitally recorded on Exabyte with the LPARL prototype OSL camera through an LPARL narrow-band (FWHM 0.3 Å) Ca II K filter that was tuned to K_{2V}. These images contain a larger field enclosing the G–band one, and were taken at regular intervals of 3.2 s. Careful alignment resulted in co-temporal and co-spatial G–band and Ca II K_{2V} image sequences, except for a brief Ca II K_{2V} data gap due to Exabyte cartridge change.

The data analysis started with dark subtractions and flat fielding. Local correlation tracking was applied to subsequent pairs of G–band frames that are 60 s apart, done on a grid with 2 arcsec spacing. It resulted in 1548 flow maps representing apparent horizontal velocities of photospheric structures within the field of view. These flow maps were averaged over time spans of increasing duration, *i.e.,* over 20, 40, and 80 min, respectively, resulting in sets of 13, 6, and 3 average flow maps.

The temporal evolution of the meso-scale flows was investigated by two different methods, which complement each other: *(i)*—calculating correlation coefficients for pairs of average flow fields with increasing time lags between the two; *(ii)*—computing trajectories of articifial "corks" (cf. Title *et al.*, 1989) for different ex-

trapolations, *i.e.*, by applying subsequent average flow maps to determine the "real" cork trajectories, and by letting corks follow the vector fields of single 20-minute flow averages for periods of up to 4 hours.

The chromospheric data are too noisy and too lacking in close-packed structure for similar local tracking and flow measurements. The Ca II K_{2V} filtergrams primarily show network and internetwork structures, with much intensity oscillation of varying signature (cf. Lites *et al.*, 1993). We have used high-speed video movies to identify the network and internetwork components by eye. An intriguing internetwork "persistent flasher" stands out in such a display (Brandt *et al.*, 1992).

3. Meso-scale flows in the photosphere

We first address the persistence of meso-scale horizontal flow patterns. Due to the short duration of most high-resolution sequences, the characteristic lifetime of meso-scale flows remains uncertain. Darvann (1991) compiled 20 analyses of meso-scale velocity and/or intensity patterning in which the lifetimes, as specified by the authors, range between several minutes and over four hours. In their recent study of mesogranular proper motions, Muller *et al.* (1992) claim a lifetime of approximately 3 hours, but their measure is only qualitative.

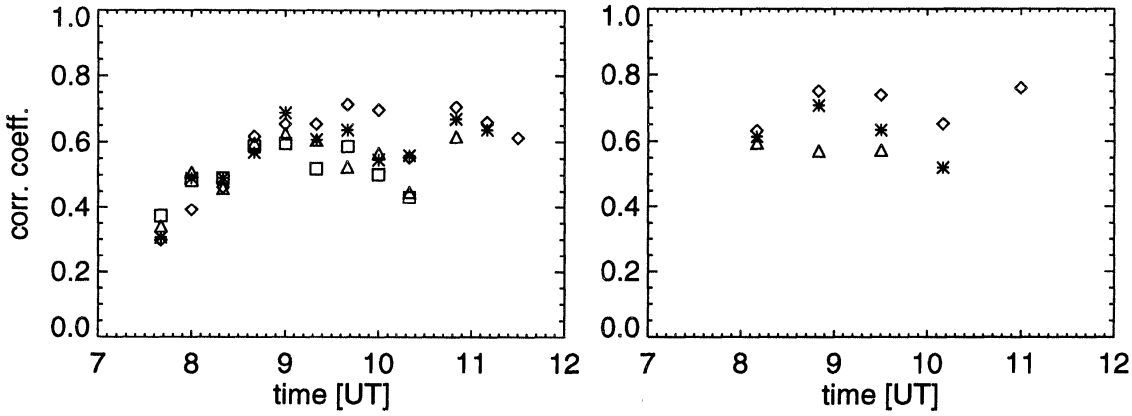

Fig. 1. Correlation coefficients between pairs of flow field averages taken at different moments against time, plotted at the time the first average was taken. Left: averages taken over 20 min, with time lags between pair members respectively 20 min (◇), 40 min (∗), 60 min (□) and 80 min (△). Right: averages taken over 40 min, with time lags of 40 min (◇), 80 min (∗) and 120 min (△).

The lefthand panel of Fig. 1 shows spatial correlation coefficients $c_{20}(\Delta t)$ between 20-min flow averages with time intervals $\Delta t = 20$, 40, 60 and 80 min, respectively. Between 07:40 UT and 09:00 UT the correlation coefficients increase from $c_{20} \approx 0.3$ to $c_{20} \approx 0.7$, staying more or less constant after 09:00 UT. In the early part of the run, the seeing was somewhat worse than later in the day; the first flow averages are therefore contaminated by larger noise which results in lower spatial correlation. The coefficients exhibit a systematic decrease with increasing time lag. It is yet clearer in the righthand panel of Fig. 1, where the flow fields are averaged over 40 minutes, and it is also present for 80-min averages (not shown).

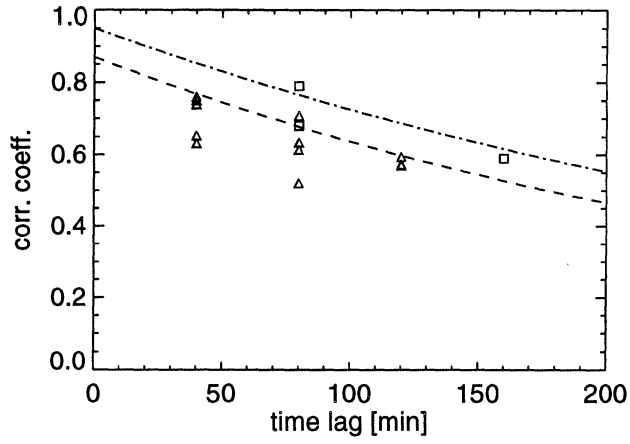

Fig. 2. Correlation coefficients between pairs of flow field averages against time lag between pair members. The averages were taken over 40 min (△) and 80 min (□), respectively. The curves are exponential fits to the highest values for each averaging span at each time lag.

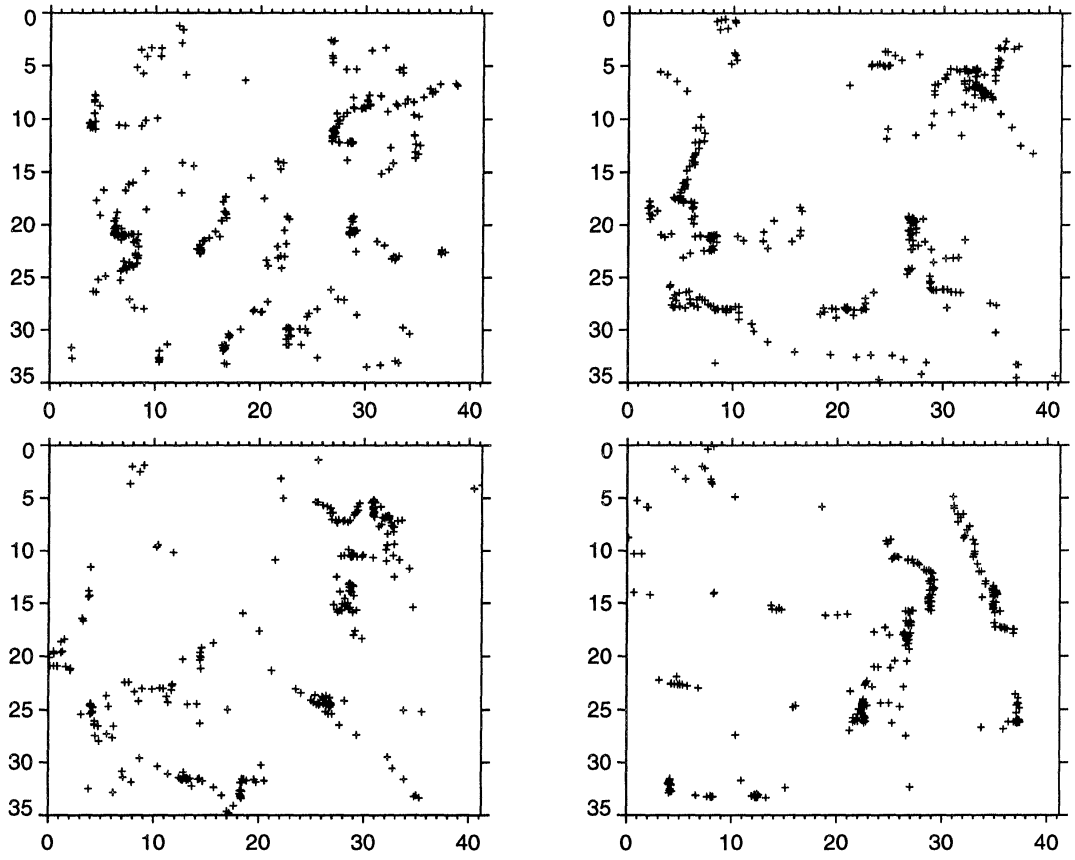

Fig. 3. Cork positions from 20-min flow averages after four hours of floating. The input flow fields were observed around 08:20 (upper left), 09:20 (upper right), 10:20 (lower left) and 11:20 UT (lower right). Axis units are arcsec (1 arcsec = 725 km on the sun).

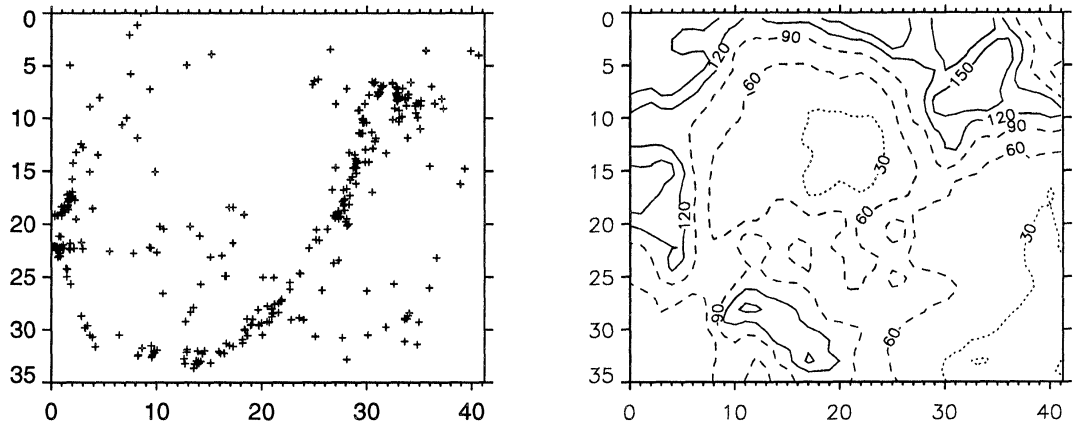

Fig. 4. Left: cork positions derived from 12 subsequent 20-min flow averages, showing the result of actual flow pattern evolution over 4 hours. The cork concentrations outline supergranulation cells. Right: isophotes of Ca II K_{2V} brightness averaged over 40 minutes. Large Ca II K_{2V} intensity outlines the chromospheric network.

Obviously, longer averaging reduces the seeing noise, but smoothes out intrinsic evolution of the flow patterns. To disentangle the two effects, we plot the correlation coefficients in Fig. 2 against lag duration for all 40-min and 80-min averages. There is some scatter at each lag; we take the highest values to represent correlation least impaired by residual seeing. Exponentials of the form $c(t) = c_0 \exp(-t/T)$ were fitted to these highest values. For the 40-min averages we obtain an $1/e$ decay estimate $T_{40} = 320$ min, for the 80-min averages $T_{80} = 370$ min. Thus, we find that the characteristic $1/e$ lifetime of these meso-scale flows is five to six hours.

An alternative (and complementary) way of visualizing the temporal evolution of meso-scale flow patterns is by the use of "corks". In the past, cork flow patterns measured on relatively brief image sequences have been extrapolated to show where they would end up eventually, would the measured flows persist for a dozen hours or more. Our sequence is sufficiently long to test such extrapolation. Figure 3 shows cork maps derived from four 20-min flow averages, at intervals of one hour. Each map shows the locations which corks, initially sprinkled uniformly over the surface, have reached after they have floated for four hours along the flow vectors defined by the given 20-min average. There is general similarity between the four patterns; however, it is quite clear that the concentrations and dilutions of corks (which represent areas of negative and positive divergence in the flow fields, respectively) vary appreciably from panel to panel. Thus, there is intrinsic evolution in the meso-scale flow pattern.

For comparison, the lefthand panel of Fig. 4 shows cork positions derived from the application of twelve subsequent 20-min flow averages, covering the observing run, to corks let loose initially on an equidistant mesh. This map represents the actual pattern evolution over four hours. It again differs substantially from the extrapolations in Fig. 3, and contains a long, curved ridge of cork concentration that would not be picked out from any of the four maps in Fig. 3. It represents the border of a supergranulation cell in the upper left part. Four hours of horizontal meso-scale transport is sufficiently long to sweep the cell interior fairly clean of corks. (Note that convergence areas close to the edges of the field may get few corks if those

should come from outside the field, where no corks are sprinkled).

The righthand panel of Fig. 4 shows the Ca II K_{2V} intensity pattern, averaged over 40 minutes to take out solar as well as seeing fluctuations. The chromospheric network is marked by bright emission; it outlines the circumference of an internetwork cell at the upper left and part of another one at the lower right. Comparison of the left- and righthand panels demonstrates that the corks tend to concentrate in and near the network. This result confirms the earlier finding by Simon *et al.* (1988) from SOUP data, but without employing temporal flow extrapolation and its attendant uncertainties (Fig. 3). Figure 4 shows *directly* that the chromospheric network results from the interplay between turbulent convection and magnetic field elements.

4. Chromospheric corks

From careful inspection of the Ca II K_{2V} sequence, displayed and blinked at high speed using optical disk storage, we have found that there are different classes of grain-like Ca II K_{2V} features present in our field of view. Bright grains in the network stand out by their positional stability, even if they come and go with characteristic periodicity of about five minutes. In the internetwork, there are fairly large areas where nothing much happens except for low-amplitude three-minute oscillations (periodicities in the 2–4 minute range), with spidery horizontal patterning, large apparent horizontal phase speeds, and rather dark low-intensity phases. In some particular internetwork areas, especially the one at the lower right in Fig. 4, there is 3–min activity with larger amplitude. It sometimes results in small, exceptionally bright emission features that presumably are the so-called Ca II K_{2V} grains much debated in the literature (see Rutten and Uitenbroek, 1991 and the contribution by Lites *et al.* in these proceedings; an example is shown by Brandt *et al.*, 1992).

A third class of Ca II K_{2V} grains is represented by a single internetwork feature, visible as an emission grain at intervals of 3 to 5 minutes, which becomes conspicuous by maintaining its identity throughout the image sequence only if that is displayed at large speed. It is then seen to travel, while flashing in and out of sight, from the center part of the upper-left supergranulation cell towards its lower boundary. Figure 5 shows a few snapshots along its path. After 10:00 UT, the feature flashes less conspicuously and has smaller proper motion. It loses identity between the network grains, which start migrating downward at about the same time. We call the migrating feature "the persistent flasher", and have shown its brightness behavior in Brandt *et al.* (1992) where we argued that such rare features (a single one in this whole sequence) may explain the correlation between broad-band Ca II K grains and magnetic flux enhancements in internetwork regions observed by Sivaraman and Livingston (1982).

The trail in Fig. 6 traces the corresponding meso-scale flow at the photospheric level. It is the trajectory of a single cork, located initially near the position where the flasher is seen at the start of the Ca II K_{2V} sequence, and then followed during four hours of flow evolution. Clearly, there is close agreement between the cork travel towards the lower supergranular boundary in Fig. 6 and the migration of the flasher towards the chromospheric network sampled in Fig. 5. Blinking between the

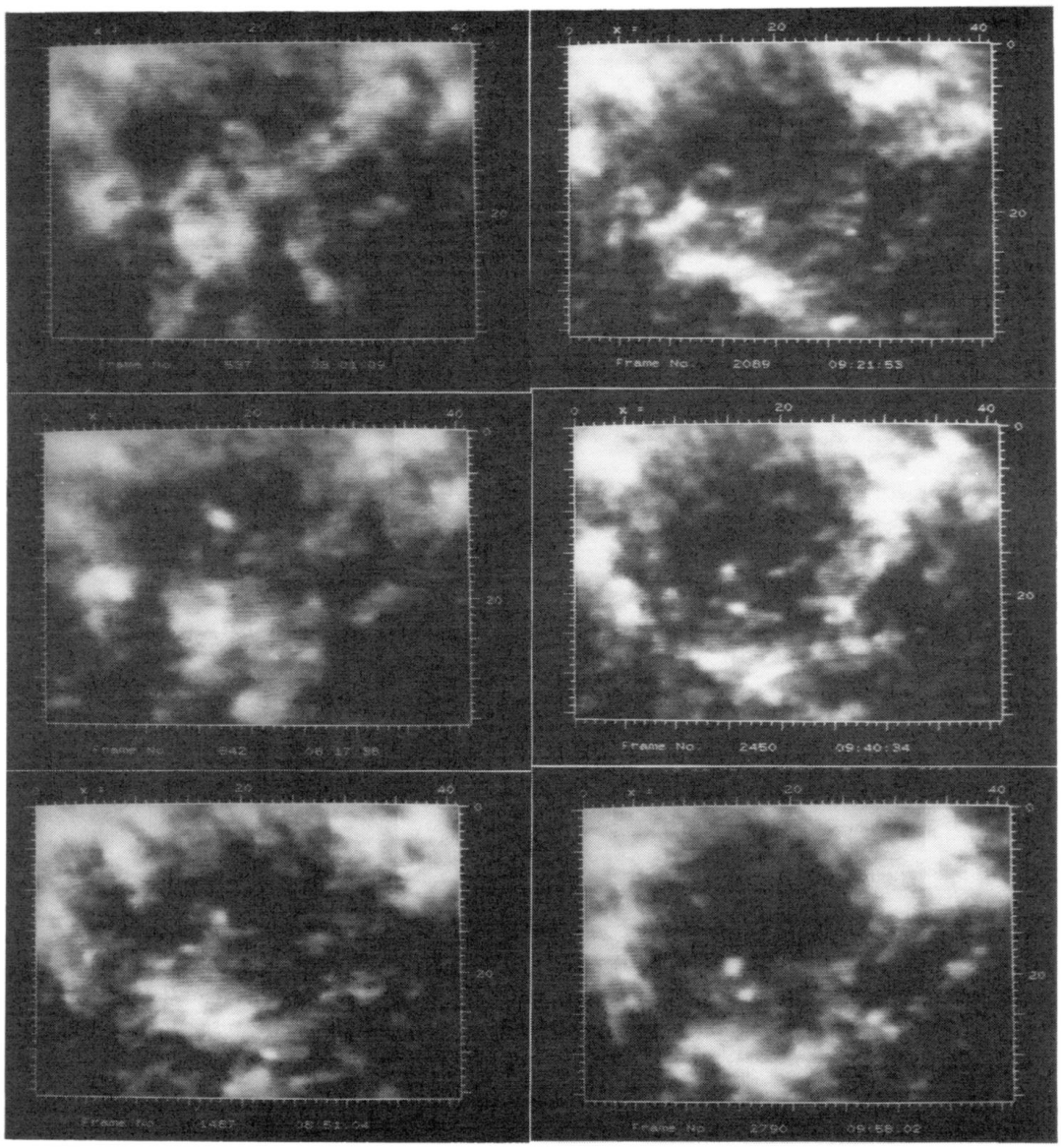

Fig. 5. Ca II K_{2V} exposures taken at 08:01 (upper-left panel), 08:17 (middle left), 08:51 (bottom left), 09:21 (upper right), 09:40 (middle right) and 09:58 UT (lower right). These were times at which the "persistent flasher" was bright. It moved from position $x = 18$ (from left) and $y = 9$ (from top) in the first panel to position $x = 14$, $y = 19$ in the last one.

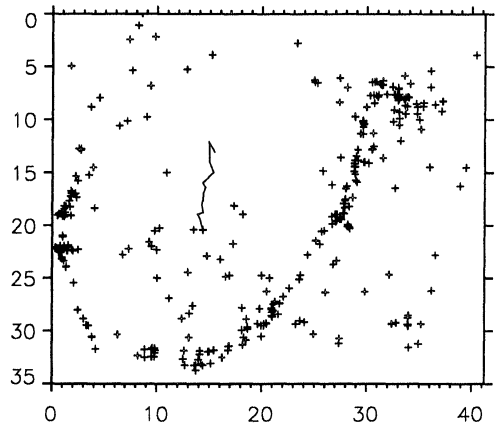

Fig. 6. Cork positions after 4 hours of evolution with the trail of one cork marked; it moves from near the center of an internetwork cell towards its lower boundary.

corresponding cork and CaII K_{2V} video movies shows the correspondence directly. Thus, the persistent flasher in the chromosphere is swept along with the meso-scale flows in the photosphere: it is a true solar cork rather than an artificial computer-generated one.

5. Discussion

The $1/e$ lifetime of 5 to 6 hours determined above for meso-scale flows is a higher value than earlier estimates, including the one by Muller *et al.* (1992), but represents a lower limit rather than an upper one. Residual noise due to seeing, if present, reduces the correlation coefficients; longer pattern persistence would probably also result if displacements of individual meso-scale elements are followed while they evolve, as done by Muller *et al.* (1992).

A significant difference between the cork topologies that result from the flow extrapolations in Fig. 3 and from the actual flow evolution in Fig. 4 is the lack of definite sink points in the latter. When corks follow fixed flow patterns for sufficiently long times, they all end up in a few centers of convergence; in reality, the solar flow patterns evolve while the corks are swept along. Image sequences of at least the duration of our data set are required to follow cork migration from the centers of supergranulation cells to their boundaries.

Our results show that both photospheric corks and the chromospheric flasher are swept to the cell boundaries. Clearly, such migration contributes to the topology of the magnetic network, seen in our CaII K_{2V} images as chromospheric network. However, it is wrong to regard this process as a one-way street. Conversely, the presence of the magnetic flux concentrations affects the convection flows. The persistent flasher is, in view of its longevity and photospheric anchoring, presumably of magnetic origin. Its arrival at the network may influence the flows that govern the local network topology.

Finally, our data sequence is more limited in both duration and spatial extent than one would like. Modern CCD camera's, non-biological image grabbing systems,

and days without Caldeira thermals as described by Simon *et al.* elsewhere in these proceedings permit the taking of vastly increased data sets. However, the quest lies perhaps not in getting better granulation sequences *per sé*, but in tying photospheric *and* chromospheric horizontal *and* vertical velocity fields *and* magnetic fields all together. Our data set shows that the simple addition of a second channel taking Ca II K images adds the chromosphere and, with K–line intensity taken as proxy, the topology of magnetic flux amplitude. An even better tactic is to alternate Ca II K narrow-band imaging between the Ca II K_{2V} and Ca II K_{2R} wavelengths as suggested by Rutten and Uitenbroek (1991), because the normalized intensity difference $(R - V)/(R+V)$ provides an excellent proxy for radial velocity in the chromosphere (Lites *et al.*, these proceedings).

Acknowledgements. We are indebted to G.B. Scharmer, R. Kever and G. Hosinsky of the Swedish Solar Observatory at La Palma for the use of their superb equipment and their support with the observations, and to Z. Frank and the late K. Smith of the Lockheed Palo Alto Research Laboratories for help with the data reduction. We gratefully acknowledge funding from NATO in the form of CRG travel grant nr. 900229.

References

Brandt, P. N., Ferguson, S., Scharmer, G. B., Shine, R. A., Tarbell, T. D., Title, A. M., and Topka, K.: 1991, *Astron. Astrophys.* **241**, 219

Brandt, P. N., Rutten, R. J., Shine, R. A., and Trujillo Bueno, J.: 1992, in M. S. Giampapa and J. A. Bookbinder (Eds.), *Cool Stars, Stellar Systems, and the Sun*, Proc. Seventh Cambridge Workshop, Astron. Soc. Pac. Conf. Series 26, p. 161

Brandt, P. N., Scharmer, G. B., Ferguson, S. H., Shine, R. A., Tarbell, T. D., and Title, A. M.: 1988, *Nature* **335**, 238

Damé, L.: 1985, in H. U. Schmidt (Ed.), *Theoretical Problems in High Resolution Solar Physics*, MPA/LPARL Workshop, Max-Planck-Institut für Physik und Astrophysik MPA 212, München, p. 244

Damé, L. and Martić, M.: 1987, *Astrophys. J.* **314**, L15

Darvann, T. A.: 1991, *Solar horizontal flows and differential rotation determined by local correlation tracking of granulation*, Cand. Sci. Thesis, University of Oslo

Deubner, F.-L.: 1989a, in R. J. Rutten and G. Severino (Eds.), *Solar and Stellar Granulation*, NATO ASI Series C-263, Kluwer, Dordrecht, p. 195

Deubner, F.-L.: 1989b, *Astron. Astrophys.* **216**, 259

Dialetis, D., Macris, C., Muller, R., and Prokakis, T.: 1988, *Astron. Astrophys.* **204**, 275

Kawaguchi, I.: 1980, *Solar Phys.* **65**, 207

Koutchmy, S. and Lebecq, C.: 1986, *Astron. Astrophys.* **169**, 323

Lites, B. W., Rutten, R. J., and Kalkofen, W.: 1993, *Astrophys. J.* **414**, 345

Muller, R., Auffret, H., Roudier, T., Vigneau, J., Simon, G. W., Frank, Z., Shine, R. A., and Title, A. M.: 1992, *Nature* **356**, 322

Muller, R., Roudier, T., and Vigneau, J.: 1990, *Solar Phys.* **126**, 53

November, L. J. and Simon, G. W.: 1988, *Astrophys. J.* **333**, 427

November, L. J., Toomre, J., Gebbie, K. B., and Simon, G. W.: 1981, *Astrophys. J.* **245**, L123

Oda, N.: 1984, *Solar Phys.* **93**, 243

Rutten, R. J. and Uitenbroek, H.: 1991, *Solar Phys.* **134**, 15

Simon, G. W. and Leighton, R. B.: 1964, *Astrophys. J.* **140**, 1120

Simon, G. W., Title, A. M., Topka, K. P., Tarbell, T. D., Shine, R. A., Ferguson, S. H., Zirin, H., and The Soup Team: 1988, *Astrophys. J.* **327**, 964

Sivaraman, K. R. and Livingston, W. C.: 1982, *Solar Phys.* **80**, 227

Straus, T., Deubner, F.-L., and Fleck, B.: 1992, *Astron. Astrophys.* **256**, 652

Title, A. M., Tarbell, T. D., Topka, K. P., Ferguson, S. H., Shine, R. A., and the SOUP Team: 1989, *Astrophys. J.* **336**, 475

Wang, H.: 1989, *Solar Phys.* **123**, 21